Towards a Switchable AR/VR Near-eye Display with Accommodation-Vergence and Eyeglass Prescription Support

Xinxing Xia, Yunqing Guan, Andrei State, Praneeth Chakravarthula, Kishore Rathinavel, Tat-Jen Cham, and Henry Fuchs *Life Fellow, IEEE*
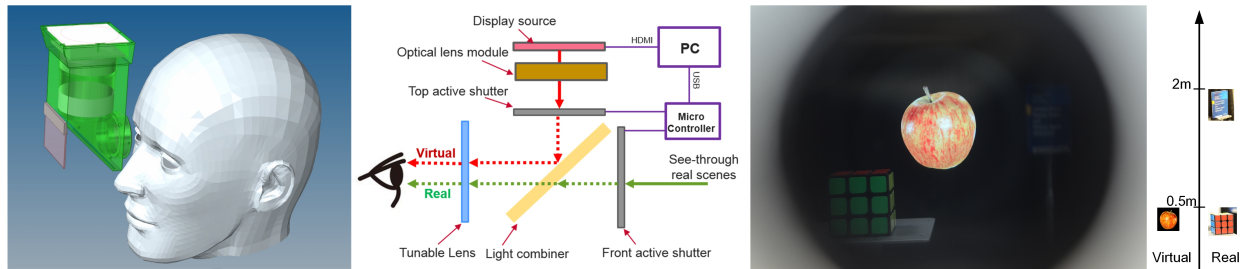

Fig. 1. Overview of our proposed time-multiplexed near-eye display with accommodation-vergence and eyeglass prescription support. *Left:* Prototype design of our proposed near-eye display. *Middle:* System diagram of our proposed near-eye display. *Right:* The view for a far-sighted user with a prescription of +0.5D looking through our proposed near-eye display without wearing his own prescription glasses. The real physical Rubik's cube is placed at 0.5m from the viewer's eye and the virtual apple is imaged at the same distance. *Extreme right:* Overhead depiction of scene geometry. The icon on the left of the optical axis refers to virtual object (apple), while the icons on the right of the optical axis refer to real physical objects (Rubik's cube and book) located at different depths.

Abstract—In this paper, we present our novel design for switchable AR/VR near-eye displays which can help solve the vergence-accommodation-conflict issue. The principal idea is to time-multiplex virtual imagery and real-world imagery and use a tunable lens to adjust focus for the virtual display and the see-through scene separately. With this novel design, prescription eyeglasses for near- and far-sighted users become unnecessary. This is achieved by integrating the wearer's corrective optical prescription into the tunable lens for both virtual display and see-through environment. We built a prototype based on the design, comprised of micro-display, optical systems, a tunable lens, and active shutters. The experimental results confirm that the proposed near-eye display design can switch between AR and VR and can provide correct accommodation for both.

Index Terms—Near-eye displays, Augmented reality, Virtual reality, Focus accommodation, Prescription correction

---

1 INTRODUCTION

A head-mounted display (HMD) [31] or near-eye display is a critical key component for both Virtual Reality (VR) and Augmented Reality (AR) technologies. For VR, a near-eye display is tasked with producing the immersive environment for the user, while a near-eye display for AR must seamlessly integrate virtual scenes into the real world, which enables and facilitates interaction between virtual and real objects.

Although significant advances in near-eye displays have been demonstrated by both academia and industry, currently reported near-eye

- *Xinxing Xia is with Institute for Media Innovation, Nanyang Technological University. E-mail: lygxia@gmail.com.*
- *Yunqing Guan is with Infocomm Technology Cluster, Singapore Institute of Technology. E-mail: frank.guan@singaporetech.edu.sg.*
- *Andrei State is with InnerOptic Technology Inc. and Department of Computer Science, University of North Carolina at Chapel Hill. E-mail: andrei@cs.unc.edu.*
- *Praneeth Chakravarthula is with Department of Computer Science, University of North Carolina at Chapel Hill. E-mail: cpk@cs.unc.edu.*
- *Kishore Rathinavel is with Department of Computer Science, University of North Carolina at Chapel Hill. E-mail: kishore@cs.unc.edu.*
- *Tat-Jen Cham is with School of Computer Science and Engineering, Nanyang Technological University. E-mail: astjcham@ntu.edu.sg.*
- *Henry Fuchs is with Department of Computer Science, University of North Carolina at Chapel Hill. E-mail: fuchs@cs.unc.edu.*

displays still have a number of issues that have not yet been solved. For example, depth perception enables human to perceive the distance of an object in the real world; in physiology, depth perception arises from a variety of depth cues, including binocular parallax, motion parallax, vergence and accommodation [10]. Most commercial near-eye displays are based on the principle of binocular parallax. It means that the near-eye display presents a stereoscopic image pair as separate images for the left and right eyes, and each eye can only observe a 2D image. This method provides only binocular parallax but no other depth cues. Also, prolonged viewing may lead to discomfort due to the vergence-accommodation-conflict (VAC) issue where the eyes converge at the apparent distance of an object but focus at the image plane of the virtual display. To solve the VAC problem, the near-eye display must provide depth cues such as pupil motion parallax and accommodation. To that end, some methods used in glass-free 3D displays are applied to near-eye display design, such as multi-view, integral imaging, light field, volumetric, varifocal, multi-focal and holographic techniques [8]. Moreover, display resolution, field of view (FOV) and form factor are also key design criteria for near-eye displays expected to enhance the human natural visual experience with seamless fusion between virtual and real scenes.

Some of the technologies aiming to mitigate the VAC problem for near-eye displays, such as light field near-eye displays, multi-view near-eye displays and integral imaging near-eye displays, usually suffer from various drawbacks, e.g. poor resolution, limited FOV and large form factor [9]. Other solutions, such as holographic displays, can solve the VAC completely, in principle, but the reported implementations are usually compute-intensive and suffer from a small eye box [24] or small FOV [7]. The solutions based on volumetric display can reconstruct the

volume in space without the VAC problem, but require high-frame-rate display devices and high-speed vari-focal optical components to sweep the display volume.

This paper presents a novel time-multiplexing method of combining virtual content and see-through real scenes in a near-eye display. A fully implemented near-eye display system based on this concept could switch between AR and VR modes and present the virtual image at a desired distance in space. This helps to successfully solve the VAC problem for both AR and VR and also helps to remove the prescription glasses for near- and far-signed users.

1.1 Contributions

In this paper, we present our novel method, which uses time-multiplexing to integrate virtual contents and see-through real scenes. As virtual contents and see-through real scenes are separately displayed in the temporal domain, tunable lenses are utilized to adjust the virtual image at the user's viewing distance such as to solve the VAC problem. Concretely, this paper's main contributions are:

1. A novel design for near-eye display which can support both AR and VR modes and mitigate the VAC issue. The proposed near-eye display could render the virtual image from 0.33m to infinity and has the potential to achieve a large FOV with larger tunable lens aperture.

2. Under time-multiplexing, virtual contents and see-through real scenes can be perceived through different optical paths and at different focus settings, without interfering with each other; thus, it helps to eliminate the eyewear for far/near -sighted and presbyopic users.

3. A prototype of the switchable AR/VR eyeglasses has been developed with off-the-shelf components, including optical lenses, an electrically tunable lens, active shutters, and an Arduino controller and micro-display; it can operate in real-time.

2 RELATED WORK

Based on the different methods for providing depth cues, near-eye displays can be divided into several categories, including binocular near-eye displays, light field near-eye displays, holographic near-eye displays, Maxwellian view near-eye displays, multifocal near-eye displays, vari-focal near-eye displays and multiplexed near-eye displays.

2.1 Binocular Near-eye Displays

Binocular near-eye displays usually present a stereoscopic image pair as individual images to each eye. It means that each eye observes only a 2D image, and depth perception is only provided by binocular parallax. Currently most commercial VR/AR products are based on binocular near-eye displays. The simplest VR display design utilizes two small LCD panels and two Fresnel lenses to create 3D perception. Binocular AR displays need a transparent combiner to integrate virtual imagery into see-through real scenes. Different types of combiners are designed to ensure that the virtual image forms at a certain distance and that see-through real scenes are not distorted. Google Glass utilizes an LCoS micro-display and a prism combined with an end reflector to create a first AR commercial product [29]. But the FOV of Google Glass is only about 15°and its prism is relatively thick. To reduce combiner thickness, the light-guide optical element (LOE) with a series of specially designed partial mirrors was proposed by Lumus, resulting in an HMD with a FOV of 35° [1]. A further improvement was achieved with the introduction of the holographic waveguide [26, 36]. It uses a pair of volume holographic gratings as separate in-coupler and out-coupler and the image is transmitted inside the waveguide by means of total internal reflection (TIR). With the holographic waveguide as combiner, near-eye display's form factors are improved considerably, but their FOV remains limited due to the theoretical TIR angle of the waveguide.

Finally, freeform optical prism combiners can yield better imaging quality with less distortion and larger FOV when compared with traditional spherical surface. Cheng et al. reported an optical see-through HMD system based on a freeform prism and with a FOV of 53.5° [5].

However, all of the above solutions only provide binocular parallax without any other depth cue, and therefore do not address the VAC problem.

2.2 Light Field Near-eye Displays

Light fields synthesize a series of light rays to reconstruct the 3D scene and provide accurate focus cues and occlusion effects. Multi-view and integral imaging displays also principally reconstruct the light rays of the 3D scenes, and can thus also be categorized as light field displays. Both solutions could be applied to near-eye displays to create a light field in the region of the pupil. They can provide accommodation for each eye and help the user assess the distance of virtual display elements. A lens array mounted in front of a micro-display panel implements a thin and lightweight light field VR display capable of presenting nearly all biological depth cues [16]. Integral imaging can be combined with existing freeform-prism-based near-eye display to solve or relieve the VAC problem [12]. The "super multi-view" method can be integrated into a near-eye display, yielding 21 views inside the pupil region to solve the VAC problem [35]. Layered LCD structures can also form a compressed light field in VR [13] and AR [23] eyeglasses, improving display image quality in the fovea based on a weighted optimization algorithm [19]. Pinlight displays present a light field solution for wide FOV AR eyeglasses with a point light source array [25]. Retinal 3D demonstrated a light field retina projection with eye tracking to generate a larger eye box [14]. However, current implementations of light field displays have poor resolution due to the trade-off of spatial and angular resolution, or are diffraction-limited due to the pinhole imaging.

2.3 Holographic Near-eye Displays

Holographic display is an ideal approach since it reconstructs the light wavefront of the display scenes, including both amplitude and phase [9]. It can also provide accurate focus cues without the VAC problem. A holographic display is diffraction-based and thus suffers from limitations in FOV, display size and hologram computation complexity. With an off-axis lens function holographic optical element (HOE) as combiner, a holographic near-eye display in eyeglass form factor can be implemented with a phase-only spatial light modulator (SLM). It has a wide FOV of around 80°, but a very small eye box [24]. Other similar bench-top or compact implementations [4, 7, 30, 40] of holographic near-eye displays also exhibit the trade-off between FOV and eye box size, which is dependent on the resolution of the utilized SLM. Therefore, a high-resolution SLM or some other modulation device is needed to improve both FOV and eye box size. The rendering of holograms for near-eye display is another key challenge. Some of the related research is focused mainly on improving digital holography calculation [4, 30]. At this time, holographic near-eye displays are not yet suitable as a basis for commercial products.

2.4 Maxwellian View Near-eye Displays

Maxwellian view near-eye displays, or retina scanning displays, can also alleviate the VAC problem. Instead of rendering 3D images with true focal cue for each eye, the Maxwellian view near-eye display presents images which are always focused regardless of the focal length of the eye. The eye is considered as the pinhole model. Therefore, the eye box is limited to the eye pupil size, which is too restrictive. Some researchers are focused on improving the eye box for Maxwellian view near-eye displays. Holographic methods were employed to achieve Maxwellian view near-eye displays with large eye boxes through scanning of the exit pupil [15, 33]. The light field method is also utilized to achieve a large eye box, but it suffers from poor resolution as in light field near-eye displays [32, 38]. To achieve vision correction for the near-/far-sighted or presbyopia users, some researchers proposed some novel designs of Maxwellian view near-eye displays with corrective lens [3] or contact lens [37]. In general, Maxwellian view near-eye

displays can alleviate the VAC problem, but cannot provide correct depth cues for a single eye.

2.5 Multifocal Near-eye Displays

Multifocal near-eye displays usually create multiple focal planes of the virtual 3D scenes and make use of high-frame-rate display devices and tunable optical components with electrical or mechanical driving [28]. With the utilization of freeform-prism-based design, high-speed deformable membrane mirror device and high-frame-rate DMD are employed to demonstrate a multifocal bench prototype with an extended depth range reaching from 0 to 3 diopters [11]. A Savart plate can be utilized to switch the optical path with different polarization states to provide multiple focal planes for a compact near-eye display [17]. A different design uses a liquid-crystal-based (LC-based) high-speed switchable lens to create multiple focal planes for near-eye display [22]. To further extend the number of the focal planes, volumetric near-eye displays were developed [27]; these display a 3D volume in space, which can provide the required accurate depth cues. All multifocal and volumetric near-eye displays need high-frame-rate display devices and some type high-speed focus-tunable lens or curved half mirror to present the 3D scenes in different focal planes, which results in relatively complex display hardware.

2.6 Varifocal Near-eye Displays

Compared with multifocal near-eye displays, varifocal near-eye displays always provide a single focal plane whose location can be changed based on the desired distance of the virtual image. Liu et al. used a liquid lens to achieve a varifocal near-eye display with the FOV of 28° [21]. Dunn and colleagues employed a see-through deformable membrane mirror to implement a varifocal near-eye display with a wide FOV of about 60°horizontally [6]. With that design, the removal of the prescription glasses was implemented for a wide range of users, enabling them to focus on both real and virtual contents [2]. Since all pixels are presented on the same focal plane, virtual pixels located out of the plane of focus must be synthetically blurred in proportion to their distance from that plane.

2.7 Multiplexed Near-eye Displays

Each of the above-mentioned solutions for near-eye displays has its own advantages and drawbacks. Multiplexing-based methods that take advantage of these solutions can improve the quality of near-eye displays. Maxwellian view and holographic solutions were time-multiplexed to improve the FOV of the near-eye display and the resolution in the fovea region [18]. Multiple display panels with different optical paths were spatially multiplexed to obtain a wide FOV and enhance foveal resolution [34]. Zhao et al. designed spatially multiplexed multiple integral imaging modules to extend the depth of field of the integral imaging near-eye display [39]. Liu et al. time-multiplexed layered-LCD-based near-eye light field display to improve both depth range and visual experience [20]. Although multiplexing-based methods provide promising solution to get high-quality visual performance for near-eye display, the systems are usually complex which may impose challenges for manufacturing. Furthermore, it is always a challenging work to achieve precise synchronization between different components deployed in the design.

3 System Overview

The system we propose here aims to mitigate the drawbacks described in Section 2 above. It also aims to solve the VAC issue and support prescription eyeglasses removal for both AR and VR. Figure 2 shows an overview of our proposed switchable AR/VR near-eye display. It consists of display source, relay lens module, light combiner, electrically tunable lens, and two active shutters. A micro LCD display panel acts as the display source, and is imaged at a certain distance in front of the user by the partial reflection of the light combiner. The electrically tunable lens is employed to magnify the virtual image and make it appear at a specifiable focal plane for the eye, which helps solve the VAC issue of the virtual scene. When the tunable lens is not under power, it becomes flat. In this state, the top active shutter blocks the

virtual image and the front active shutter allows the see-through real scene image to pass through without aberration or distortion. When the tunable lens is under power and is able to dynamically change focus, the top active shutter will allow the virtual image to pass through and the front active shutter will block the see-through real scene image such that the eye will only perceive the virtual image. The red and green dashed lines in Figure 2 symbolize the modulated light from virtual display and see-through real scene image respectively. The front active shutter can be also turned off to block all see-through light, effectively implementing a VR display mode. The tunable lens and the two active shutters are precisely synchronized to ensure that both virtual image and real environment are observed clearly and without interference. With this time-multiplexed design, the proposed near-eye display supports both AR and VR and can help solve the VAC problem.
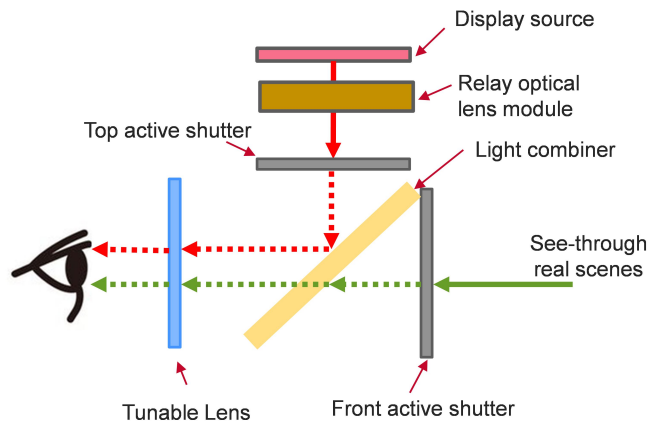

Fig. 2. An overview of the proposed switchable VR/AR near-eye display designed to address the VAC problem.

The optical design of the proposed near-eye display is detailed in Section 4, and its temporal multiplexing and synchronization strategy are discussed in Section 5. Implementation and experimental results are presented and analyzed in Section 6.

4 Optical Design

Popular VR displays usually employ a micro-display panel and a Fresnel lens for projecting to each eye. The Fresnel lens is utilized to magnify and virtually place the micro-display at a greater distance. The focal length of the lens, together with the distance between the micro-display and the lens, determine the location of the perceived image plane. For AR displays, a half mirror is inserted in the space between the lens and the eye in order to combine the virtual content and see-through real environment, as shown in Figure 3(a). The distance from the eye to the center of the combiner is denoted l_1, while the
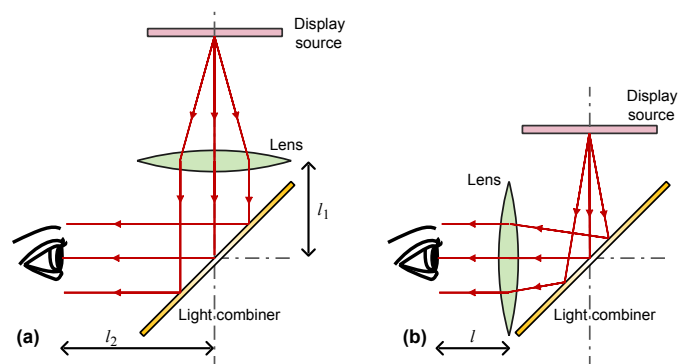

Fig. 3. Comparison with different designs of lens locations.
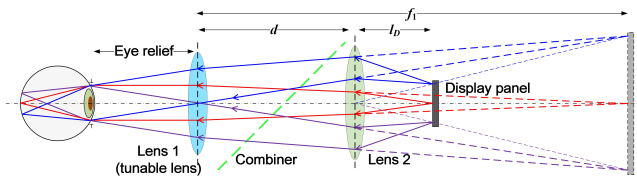
Fig. 4. Basic optical design of our near-eye display system.

distance from the center of the combiner to the lens is l_2. The distance between the eye and the lens is thus $l_1 + l_2$, which is larger than a typical VR display due to the presence of the combiner. The FOV of this setup is mainly dependent on the lens aperture D and the distance between the eye and the lens, with the maximum FOV expressed as $2\arctan(D/(2(l_1 + l_2)))$. Consequently, an AR display usually has a smaller FOV than a VR display. One approach to increasing the FOV is to have a larger lens aperture, but this will also increase the form factor of the display. The other solution is to insert the combiner into the space between the display source and the lens as shown in Figure 3(b). This design brings the lens closer to the eye, with the potential for a wider FOV, and the total length of the optical path is shorter than the design in Figure 3(a). Here the maximum FOV may be expressed as $2\arctan(D/(2l))$, which is significantly larger than for Figure 3(a). However, as the real environment is also seen through the lens, it will be magnified and distorted.

To solve this problem, we propose a mechanism to time-multiplex the virtual display and see-through real scene, using a tunable lens which can rapidly change its focal length in real time. During the time intervals when the virtual display is visible to the eye, the focal length of the tunable lens is set to virtually place the displayed image at the desired depth. During the other intervals, the tunable lens is adjusted to act as a flat plate, thus allowing the real scene to be observed without distortion. Through rapid time multiplexing, the eye will perceive the virtual image embedded at the appropriate depth within the undistorted real scene.

In our design, an Optotune electrical tunable lens is utilized; we chose the Optotune model EL-16-40-TC with a $\Phi 40$ mm$\times 11.9$ mm size and a clear aperture of $\Phi 16$ mm. This model has an optical power range of -2 to +3 dpt. When the eye relief (l) is 15 mm, we are able to achieve the maximum FOV which is around 56°. However, it is important to note that when the maximum FOV is achieved, the eyebox size is limited. In order to enlarge the eyebox, the FOV has to be reduced accordingly. The following equation defines the relationship between eye relief, FOV and the eyebox:

$$D_{eyebox} = D - 2\arctan\left(\frac{\theta_{FOV}}{2}\right)l_e \qquad (1)$$

where, D_{eyebox} is the diameter of the eyebox, D is the diameter of the clear aperture of the tunable lens, and l_e is the eye relief. Thus with an eye relief of 15 mm and an eyebox of 6mm, the FOV of the near-eye display is reduced to around 37°.

Since the nearest focus of the electrical tunable lens is 333mm, the physical display should be placed at this distance to ensure the perceived virtual image can be located up to infinity. In order to maximize display FOV in this setup, the diagonal size of the display has to be 222mm, which in conjunction with the 333mm optical path length, is not suitable for the form factor of a near-eye display. Therefore, we introduce another lens to relay the image from the micro-display to the tunable lens in order to reduce the total optical path length, and the basic optical design is shown in Figure 4 (the combiner paths are unfolded for clearer illustration). Note that the display panel is closer to lens 2 than its focus, so the display panel is seen as a virtual image at the nearest focal plane of the tunable lens.

From the geometry, the following equation holds:

$$\frac{1}{f_1 - d} + \frac{1}{l_D} = \frac{1}{f_2} \qquad (2)$$

where f_1 denotes the nearest focal length of tunable lens, f_2 the focal length of the lens 2, l_D the distance between display and lens 2, and d the distance from lens 1 to lens 2 through the combiner. The magnification of the lens 2 is:

$$M = \frac{f_1 - d}{l_D} \qquad (3)$$

In our design, we set d as 50mm and use an off-the-shelf 2.89in micro-LCD with a 1440×1440 resolution. Thus the magnification M of lens 2 is 3.0. We also calculate l_D and f_2 to be 94.3mm and 70.8mm respectively. Hence the optical path length from the display panel to the tunable lens is reduced from 333mm to 144.3mm.

To implement the optical design shown in Figure 4, we used off-the-shelf standard lenses from Edmund Optics, and also optimized the optics design using Zemax software. The radii of the spots for the different fields are smaller than or equal to the pixel size of the LCD. The detailed layout of the optics is shown in Figure 5. A concave lens and an achromatic lens (shown in the dashed pink box) constitute the relay lens module that takes the role of lens 2.
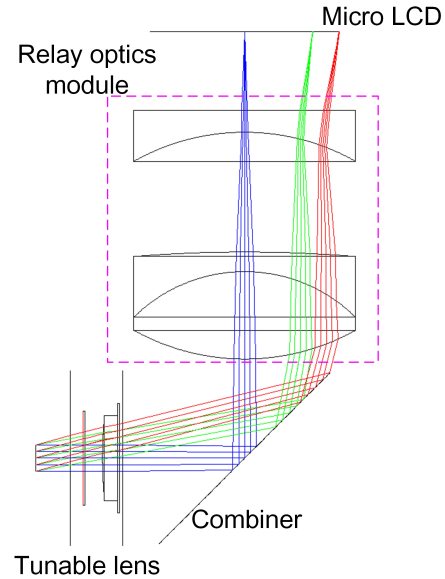

Fig. 5. Optics layout of our near-eye display system.

To alleviate the VAC, the focal length of the tunable lens can be changed to form the virtual image at different depths. Assuming the optical power linear step of the tunable lens is $\Delta\phi$, the number of discrete virtual depth layers N is $\phi_{max}/\Delta\phi$, where ϕ_{max} is the maximum optical power of the tunable lens equal to $1/f_1$. When the optical power of the tunable lens is set to $i\Delta\phi$, the virtual image at i-th layer is located at:

$$z_i = \frac{1}{\phi_{max} - i\Delta\phi} = \frac{f_1}{1 - i\Delta\phi f_1} \qquad (4)$$

and the corresponding magnification of the i-th layer is:

$$M_i = \frac{1}{1 - i\Delta\phi f_1} \qquad (5)$$

It can be observed from equation 4 that the thickness of each depth layer is different, with a smaller thickness at closer range. This means the depth resolution is higher when the virtual image is set closer to the eye, and vice versa. Since the designed FOV is 37°and the resolution of

the micro-display is 1440×1440, the angular resolution of the near-eye display is therefore around 1.54', close to the human visual acuity of 1'.

5 TEMPORAL MULTIPLEXING AND SYNCHRONIZATION

5.1 Temporal Multiplexing Pipeline

Our proposed near-eye display uses time-multiplexing to allow the user to perceive the virtual imagery and the see-through real environment. In our design, two active shutters are employed for accurate synchronization when multiplexing between the virtual display and real scene. One active shutter is placed directly in front of the user's eye to control the visibility of the real scene, while the other shutter is inserted into the optical path after the optical lens module, for accurately controlling the visibility of the virtual image. The detailed framework is presented in Figure 6.
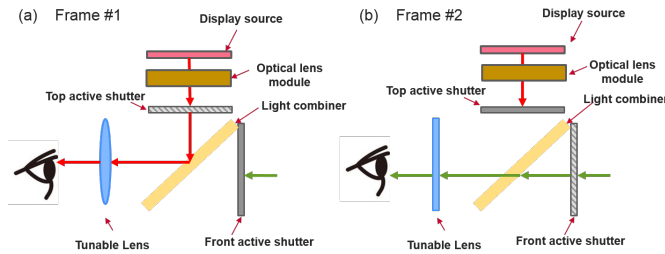

Fig. 6. Framework of near-eye display with time-multiplexed virtual display and real see-through real scenes.

Figures 6 (a) and (b) illustrate the operating details of the two shutter frames for alternating the visibility of the virtual imagery and see-through real environment. In this design, the display source for the virtual image is always on. In the first frame, the top active shutter for the virtual display is open, so the virtual image is visible to the eye. In the same instance, the front active shutter is closed to block light from the real environment. Meanwhile, the focal length of the tunable lens is adjusted to form a virtual image at the desired distance. In the second frame, the top active shutter for the virtual image is closed to block the display source, and the front active shutter is switched to the open state to allow the real environment to be seen by the user. At the same time, the focus of the tunable lens is adjusted to infinity, so that it behaves as a flat glass plate. In the AR mode for this near-eye display, both frames need to be alternated in sequence, so that the user can perceive both the virtual and real images. If the front active shutter remains closed throughout with the top active shutter open, the near-eye display goes into a VR mode.

5.2 Synchronization Strategy

For our proposed system, synchronization between the electrical tunable lens and the pair of active shutters is crucial, directly determining the display quality. Since the virtual image and see-though real scene are multiplexed, the tunable lens has to swap between two states. In one state it is a lens with focus appropriate for displaying the virtual image, while in the other state it becomes a flat plate for seeing the real scenes. During actual usage of the tunable lens, while the input signal of the lens is a rectangular wave, the optical power graph for the lens is not rectangular due to a finite rate of response. Therefore, the synchronization between the tunable lens and active shutters should be carefully crafted with consideration for the response curve of the tunable lens. To do so, we developed an effective synchronization strategy based on our system design, with the details of synchronization timing shown in Figure 7.

The top blue rectangular waveform in Figure 7 shows the driving signal of the tunable lens, and the dashed blue waveform shows the actual optical power of the tunable lens. We divided one cycle to 4 periods: t_1, t_2, t_3, and t_4. In one cycle, t_1 and t_3 represents the rising and falling periods of the optical power respectively. In the other
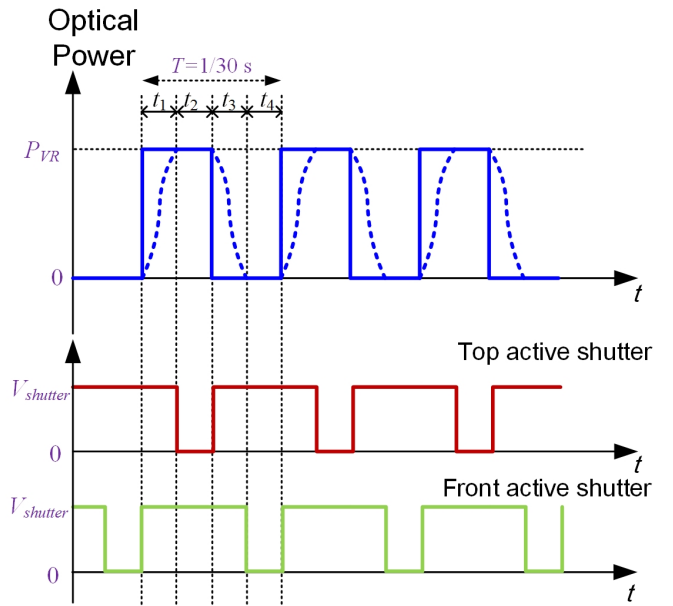

Fig. 7. Timing diagram of the synchronization between tunable lens and two shutters.

periods of t_2 and t_4, the optical power remains at P_{VR} and 0 respectively. These steady periods of t_2 and t_4 are the effective ones for our time-multiplexed near-eye display. Therefore, the active shutters are both shut during the transition periods of t_1 and t_3. We utilize LC-based active shutters in our design which are fast enough to switch between open and close states. In one cycle, the top shutter for the virtual image needs to be open in the period of t_2, while the front shutter for the see-through real environment needs to be open in the period of t_4. In practice, the duration of the four periods of t_1 to t_4 can be measured through light sensors and cameras. Based on the response time of the tunable lens, we chose a 30Hz frame rate for switching between the optical power states, and set open 25% of each frame for the top and front active shutters respectively to avoid the crosstalk between two optical states of tunable lens.

6 IMPLEMENTATION

6.1 Overview and System Configuration

To test our concept, we built a prototype for a monocular near-eye display; its system configuration is shown in Figure 8. The PC renders
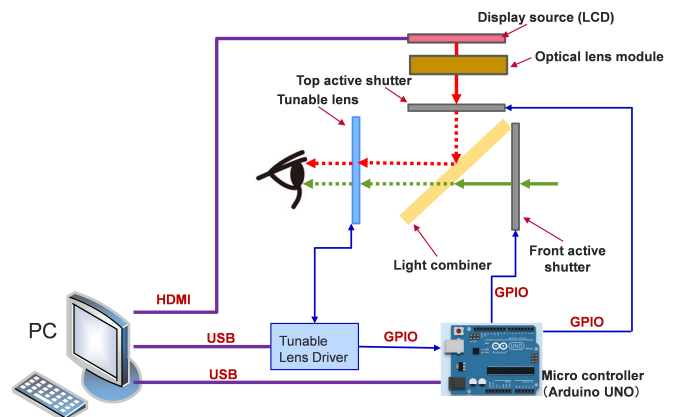

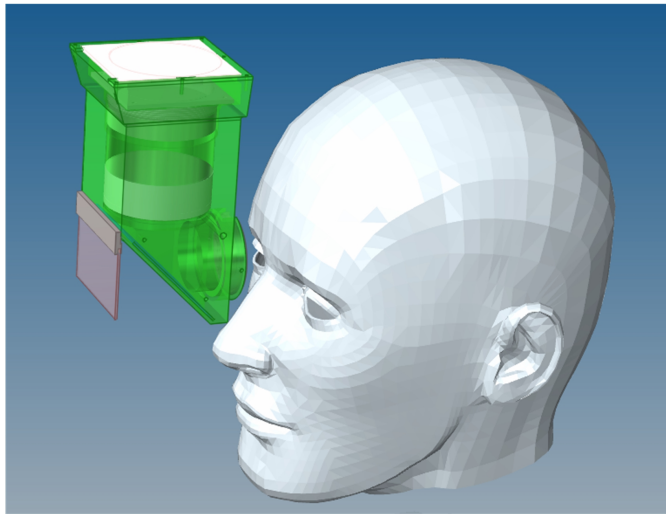Fig. 8. System diagram of the near-eye display prototype.

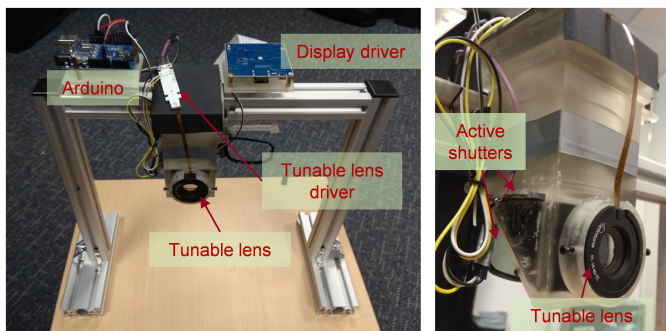Fig. 9. Design for a wearable prototype based on our proposed near-eye display.

Fig. 10. Experimental setup for our proposed near-eye display prototype whose diagram is described in Figure 8.

virtual imagery to an HDMI-connected micro-display with the resolution of 1440×1440. The active shutters were taken from off-the-shelf active 3D glasses. The optical power of the Optotune EL-16-40-TC tunable lens is controlled by a rectangular wave electrical signal output from the PC; the tunable lens also outputs sync signals when its state start to change. The sync signal from the tunable lens is sent to an Arduino micro controller (Arduino UNO) which controls the on-off state of the two active shutters, together with the pre-measured delay between the sync signal and the stable optical power change of the tunable lens. The details of the synchronization are described in Section 5.2, and the timing of two active shutters and tunable lens is shown in Figure 7.

Following the optics design shown in Figure 5, we designed an enclosure to hold lenses, micro display, active shutters, light combiner (half-silvered mirror) and tunable lens, as shown in Figure 9. The total size of the display prototype is about 54mm×60mm×122mm.

The enclosure was fabricated using a 3D printer, and the completed near-eye display prototype is mounted on an aluminum profile frame as shown in Figure 10. In our experimental setup, the eyeglasses frame of the commercial active shutters is employed to hold the active shutter as their shape is somewhat irregular.

6.2 Accommodation Experiments

Our near eye display can be switched between VR and AR modes by simply controlling the front active shutter via the micro controller. We tested it in both modes, using a resolution test chart to check image quality. We mounted a camera at the eye position to capture the image. For each mode, we presented the virtual image at different depths;

Figure 11 shows photos of these tests. In the left column, the virtual image is displayed at a distance of 0.33m and the camera is focused at the same distance. In the right column, the virtual image is displayed at a distance of 3.5m, with the camera focused at the same distance. The top row corresponds to the VR mode, showing only the resolution test chart, and the bottom row corresponds to the AR mode, showing both the resolution test chart and the see-through real scene. For the VR mode results, the resolution test chart is seen without blur at both imaging distances. For the AR mode results, one can easily distinguish the depth of the virtual image relative to the real objects, located at different depths (the Rubik's cube is at 0.33m and the poster is at 3.5m).

In a second experiment designed to verify the accommodation capabilities of our near-eye display, we use the image of a virtual apple model and display it at three different distances. For reference, we put three real objects at different distances (Figure 12): a Rubik's cube (0.33m), a book (1m) and a poster (3.5m). The camera is used to simulate the eye looking through our near-eye display and is focused at the three distances for comparison. The first column in Figure 12 shows the perspective images of the virtual apple displayed on the micro-LCD for the three distances. The first row corresponds to the image of the virtual apple displayed at distance of 0.33m where the Rubik's cube is placed. The second row corresponds to the image of the virtual apple displayed at a distance of 1m where the book is located. The last row corresponds to the image of the virtual apple displayed at distance of 3.5m where the poster is located. Each column represents images photographed with different focus settings. When the virtual apple is located at the camera focus distance, the virtual apple and the corresponding reference real object are both in focus (sharp). When the virtual image is not displayed at the camera focus distance, the observed virtual image is out of focus (blurry). These results verify that our proposed near-eye display is able to control the distance of the virtual image displayed, allowing it to fuse well with see-through real scenes. Thus, the display can help solve the VAC issue.

6.3 Optical Prescription Compensation Experiments

Most current commercial near eye displays are designed for users with normal vision. Far-sighted, near-sighted and presbyopic users must wear their own prescription eyeglasses to experience VR and AR clearly. This is frequently inconvenient for these users and can reduce the quality of their experience. Our near-eye display prototype can compensate for the optical prescriptions of such users by seamlessly integrating their prescription with the optics of the near-eye display.

To that end, the control of the tunable lens is altered such that its final optical power P after compensation is:

$$P = P_{Normal} + P_{Prescription} \qquad (6)$$

In the above equation, P_{Normal} is the optical power of the tunable lens for normal vision, and $P_{Prescription}$ is the optical power of the prescription lens for the user's eye.

For users with normal vision, the optical power of the tunable lens switches between P_{VR} for virtual imagery and 0 for see-through real scenes as shown in Figure 13(a). The frequency of the tunable lens is 30Hz.

For near-sighted users, the received light will focus in front of, instead of on, the retina. This blurs distant objects while close ones appear in focus. To extend the focus to the retina, a negative corrective lens is needed (corresponding eyewear lenses are usually concave-convex negative meniscus lenses). For our near-eye display, the function of the negative lens can be integrated into the tunable lens; the final timing of the tunable lens is as shown in Figure 13(b). The control signal waveform is simply shifted down by the optical power of the prescription lens.

For far-sighted users, the received light will focus behind instead of on the retina. This blurs close objects while distant ones are in focus. To shorten the focus to the retina, a positive corrective lens is needed (corresponding eyewear lenses are usually concave-convex positive meniscus lenses). For our near-eye display, the function of the positive lens can also be integrated into the tunable lens; the timing of the tunable lens after compensation is shown in Figure 13(c), where
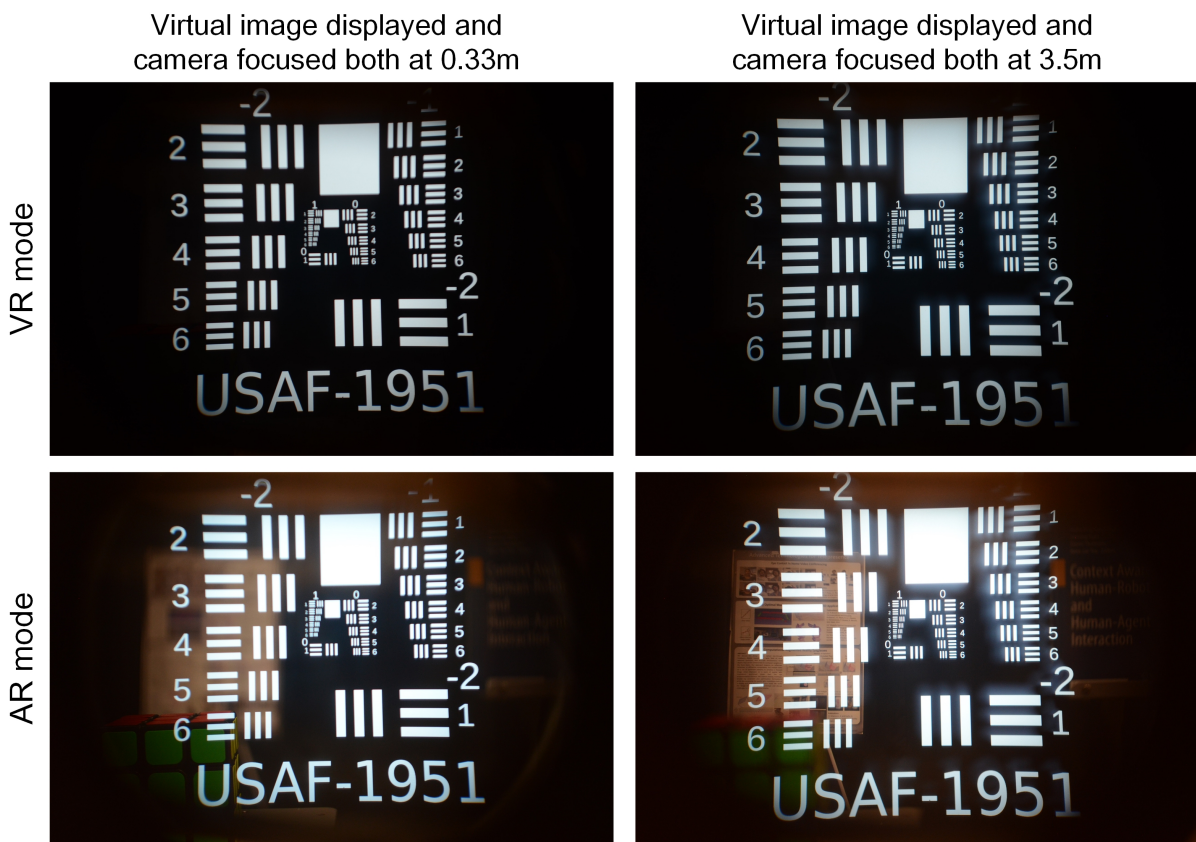
Fig. 11. Views through our near-eye display prototype in VR and AR modes, with the USAF-1951 resolution test chart shown on the micro-LCD.
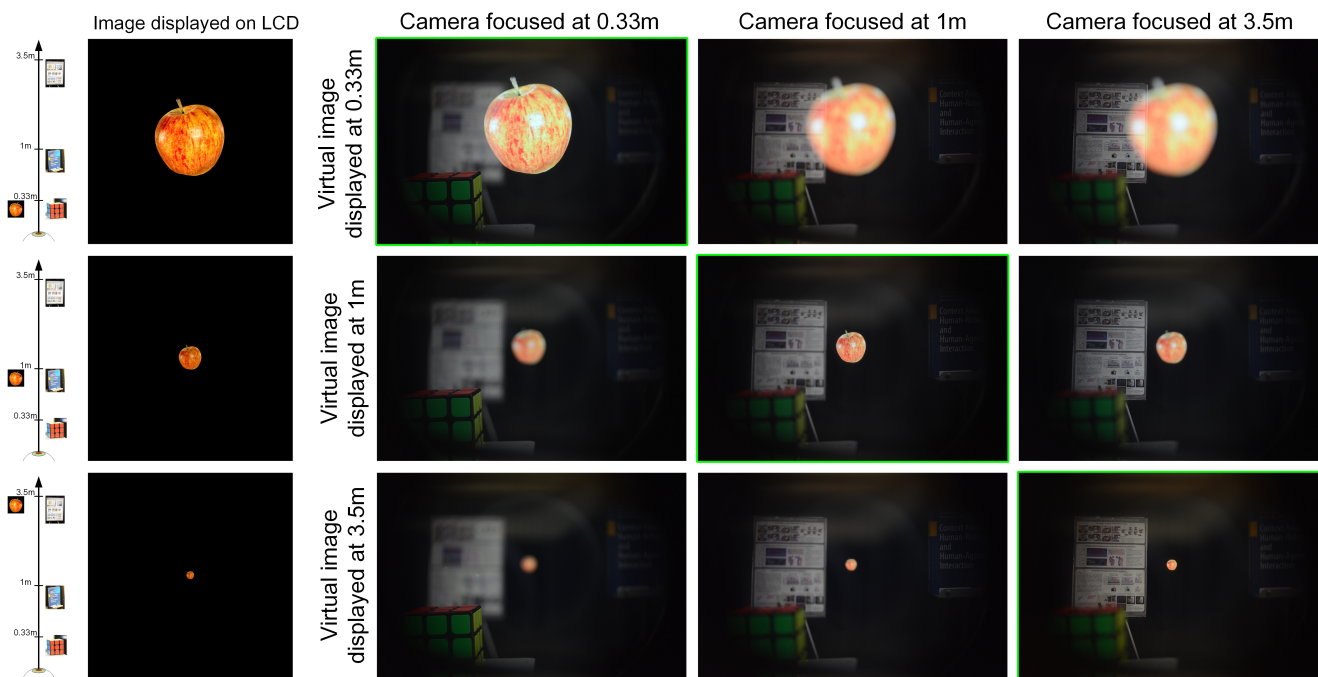

Fig. 12. Views through our time-multiplexed near-eye display, with a virtual object placed among real objects at a range of distances. Extreme left: Overhead depiction of scene geometry. Icon left of the optical axis corresponds to virtual object (apple), while icons to right of the optical axis correspond to real objects (Rubik's cube, book, poster) located at different depths.
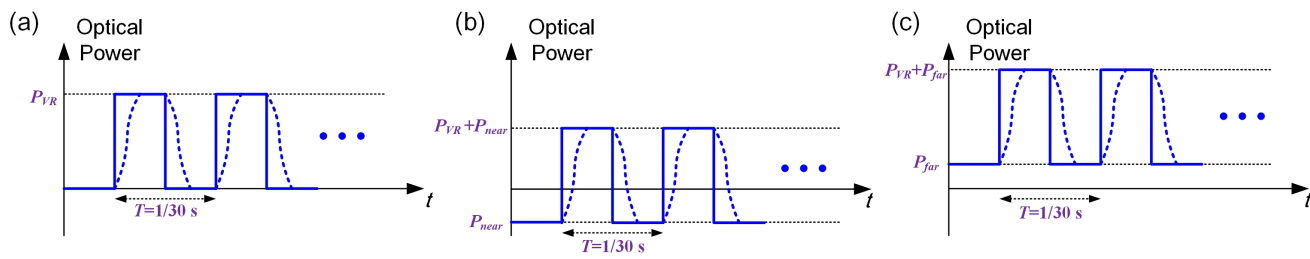
Fig. 13. Operation of the tunable lens for optical prescription compensation. (a) Timing of optical power of the tunable lens for normal vision; (b) Timing for a near-sighted user; (c) Timing for a far-sighted user.
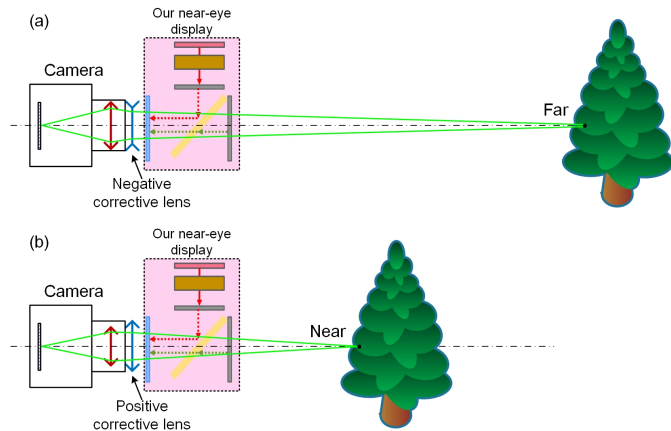

Fig. 14. Camera with prescription lens to simulate near- and far-sighted users. (a) Negative corrective lens for near-sightedness; (b) Positive corrective lens for far-sightedness.
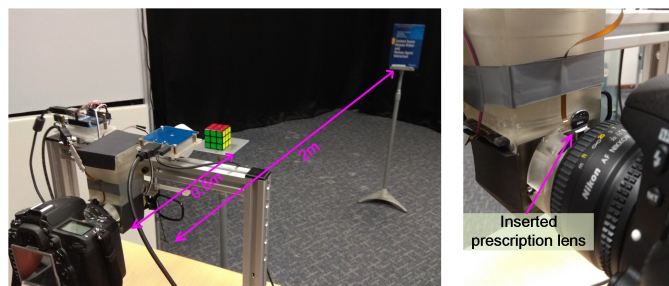

Fig. 15. Experimental setup for optical prescription compensation.

the waveform is shifted up by the optical power of the far-sightedness prescription.

For verification, we placed a prescription lens in front of the camera to simulate near- and far-sighted users. The diagrams in Figure 14 (a) and (b) show the camera as combined with negative and positive corrective lenses respectively. To approximate near- and far-sightedness respectively, we adjust camera focus to get a sharp image at a desired distance and then fix the focus setting.

Figure 15 shows the experimental setup for compensating for an optical prescription with the tunable lens. Two objects (a Rubik's cube at 0.5m and a book at 2m) are used as the reference real objects. A corrective prescription lens can be inserted between the camera and our near-eye display prototype.

We set the near-eye display in AR mode, displaying the image of the virtual apple at the distances of the two real objects respectively. A -0.5D corrective prescription lens was inserted for near-sighted users, whereupon we focused the camera to get a sharp image for both virtual

apple and corresponding reference object, as shown in the left column of Figure 16. Then we fixed the camera's focus and removed the prescription lens, which approximates the near-sighted user without corrective eyeglasses. Photos captured for the virtual and real objects at two distances (center column) show that image quality decreases in comparison with the photos captured with the corrective lens. Then we applied the -0.5D correction to the tunable lens. After that, images of the virtual apple and of the corresponding reference object (right column) are of a quality close to that of the photos captured with the corrective lens (left column). In particular, the improvement at 2m is more significant than at 0.5m, which is similar to natural viewing for near-sightedness.

To verify prescription compensation for far-sighted users, we inserted a +0.5D corrective prescription lens and performed the testing in the same manner. Figure 17 shows that the images obtained with the tunable lens replacing the prescription lens (right column) are comparable in quality to the ones photographed with the prescription lens in place (left column).

The reason for using ± 0.5D standard prescription lenses in the above-mentioned experiments of prescription compensation was due to the consideration that the compensation range of the tunable lens is not large. As near-sighted users are more sensitive to far objects while not sensitive to the near objects, and far-sighted users are more sensitive to near while not sensitive to far with correction lens, it can be observed that the results in second row of Figure 16 and first row of Figure 17 show more noticeable difference for our compensation experiments.

Presbyopia is a condition normally associated with aging. Due to hardening of the aging eye lens, light rays from close objects focus behind rather than on the retina. The correction method is similar to far-sightedness, but may need multifocal lenses to focus on objects at different distances. In our system, we can operate the tunable lens as for far-sightedness, then dynamically adjust the shift amount of the optical power of the tunable lens such that it can present both the virtual and real image at different distances in focus for users with presbyopia.

FocusAR [2] utilizes a tunable lens for prescription compensation and a deformable membrane beam splitter for varifocal virtual imagery. Compared with FocusAR, the method in our system is much easier to implement, with a single tunable optical device supporting varifocal virtual imagery as well as optical prescription compensation, for both virtual imagery and see-through real scene. FocusAR only employs one deformable membrane beam splitter to form a virtual imagery of the micro-display at different depths. Due to this simple optical design, the distortion and some other optical aberrations are obvious, and the distortion and aberration corrections must be considered in rendering pipeline to get better image quality. But in our proposed system, the design of relay optics module combing the tunable lens are optimized to get high-quality virtual imagery with less distortion and aberrations. So, the distortion and aberration corrections are almost not required to consider in the rendering pipeline of our proposed near-eye display system.
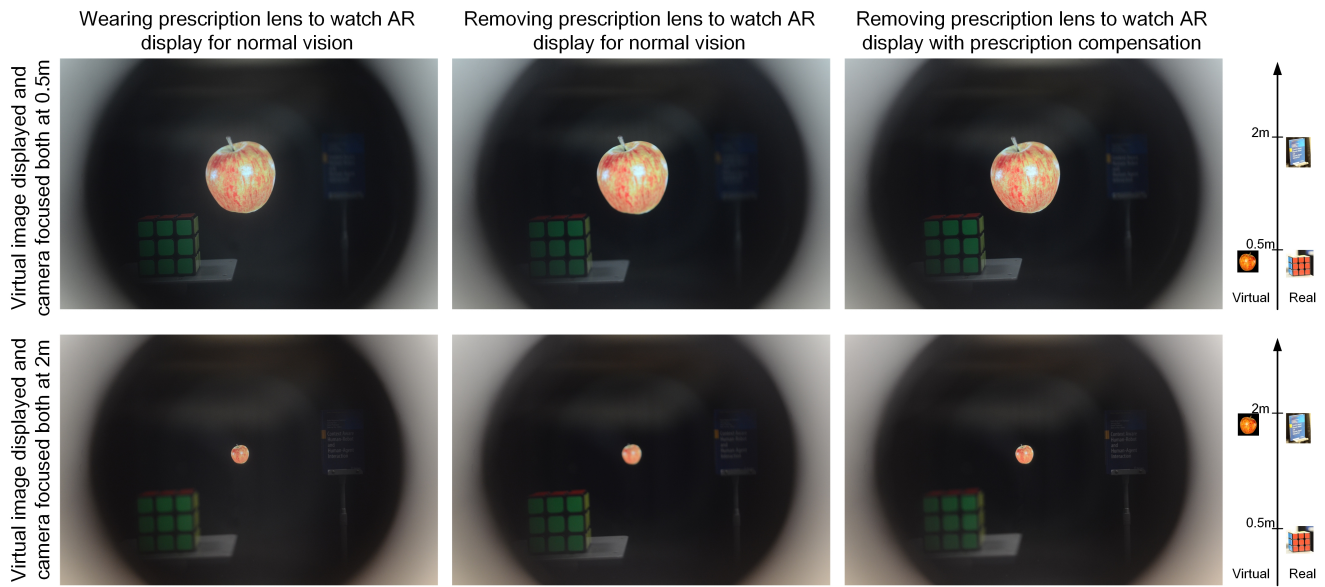
Fig. 16. Optical prescription compensation AR experiments for a near-sighted user with a prescription of -0.5D; the virtual apple is located at 0.5m (top row) and at 2m (bottom row).
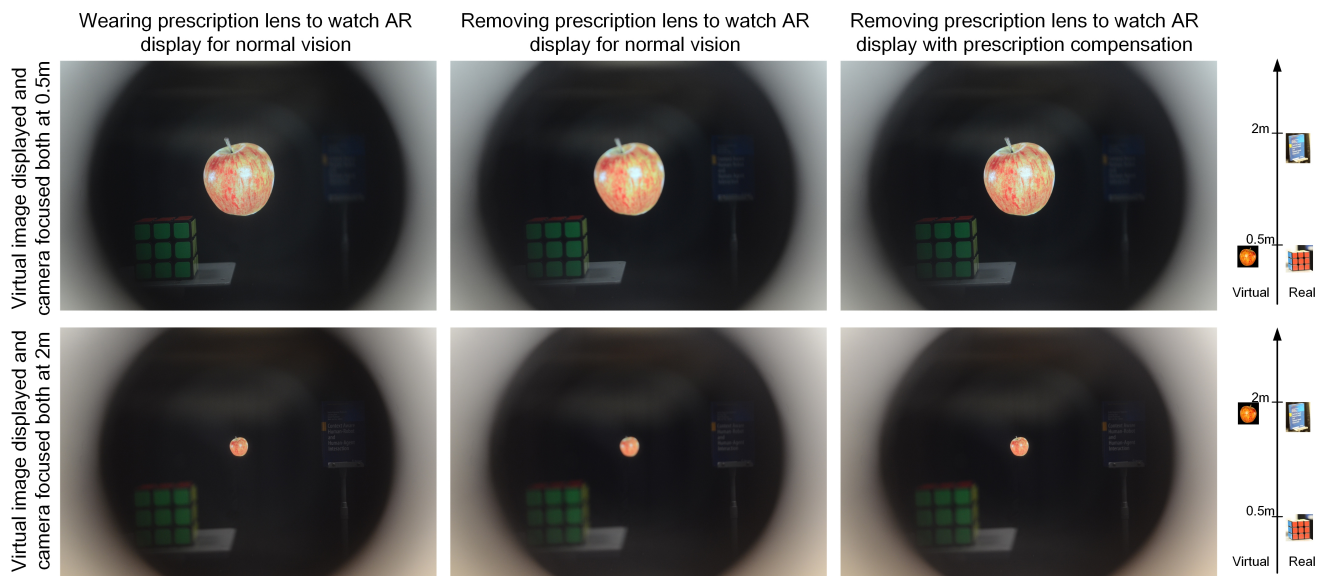

Fig. 17. Optical prescription compensation AR experiments for a far-sighted user with a prescription of +0.5D; the virtual apple is located at 0.5m (top row) and at 2m (bottom row).

7 DISCUSSION

7.1 Limitations

An advanced near-eye display should be able to support augmented imagery over a wide FOV on the order of 100°and not occlude the user's peripheral vision. The calculated diagonal FOV of our near-eye display is about 37°, constrained mainly by the aperture of the tunable lenses currently on the market. With new larger-aperture tunable lenses to be launched in the near future, the FOV can be increased. In our experiments, the limited aperture of tunable lens with its own frame also leads to a vignetting artifact which occurs at the boundary of the observed images. It can be also improved with new larger-aperture tunable lenses in the near future.

Flickering and darkening are important considerations in the design of near-eye displays. In our design of the proposed time-multiplexed near-eye display, 30Hz was chosen as the frequency for the tunable lens mainly for ensuring sufficient time for the two optical power states for both real and virtual content. Another consideration is the noise of the tunable lens with its frequency set to a higher value. As our developed near-eye display system is a proof of concept, it should be possible to raise its operating frequency in the next few years using faster tunable lenses. The top and front active shutters are set open 25% each frame of 1/30s to avoid the crosstalk between the virtual and real images, considering the transition time between the two optical states of the tunable lens. The dimness for the virtual image can be mitigated by stronger LCD backlight and we have experimented with 3-4x backlight brightness increase. Dimness for real-world images is more serious, but acceptable when compared to wearing sunglasses, which commonly may pass about as little as 20% of the incoming light. With new higher-frequency tunable lenses with less transition time to be launched in the near future, the flickering and darkening issues can be solved fundamentally.

7.2 Future Work

We plan to integrate eye tracking technology to capture the gaze direction of the user's eyes such that the optical power of the tunable lens can be adjusted in real time to make the virtual image displayed dynamically at the vergence distance.

To minimize crosstalk between virtual and see-through imagery in our current design, only about one quarter of one frame time is used for each of these two image sources, reducing the brightness of the see-through real environment. To increase brightness, we will explore doubling the display time for see-through imagery within one frame time by using only the front active shutter to control visibility of the see-through real scene images. The top active shutter for virtual content can then be removed, and this can be achieved when the display source, tunable lens and front active shutter could be synchronized using the sync signal output by the display source, i.e. the PC graphics card.

8 Conclusion

We have demonstrated a novel design for switchable VR/AR near-eye displays that can help solve the VAC issue. We use time-multiplexing to integrate virtual image and real environment visually, combined with a tunable lens that adjusts focus for virtual display and see-through real scene separately. A prototype of the proposed near-eye display was developed with off-the-shelf optical lenses, an electrically tunable lens, commercial active shutters, an Arduino controller and a micro-display. The experimental results show that the proposed near-eye display design can successfully switch between VR and AR and provides correct accommodation for both VR and AR, thus solving the VAC issue. With this novel design, prescription eyeglasses for near- and far-sighted users are unnecessary as the optical prescription can be taken into account by the tunable lens for both virtual display and see-through real scene. This was verified experimentally for both negative and positive prescription lenses.

Acknowledgments

References

[1] Y. Amitai. Light guide optical device, nov 2008.

[2] P. Chakravarthula, D. Dunn, K. Aksit, and H. Fuchs. FocusAR: Autofocus augmented reality eyeglasses for both real world and virtual imagery. *IEEE Transactions on Visualization and Computer Graphics*, 2018. doi: 10.1109/TVCG.2018.2868532

[3] C. P. Chen, L. Zhou, J. Ge, Y. Wu, L. Mi, Y. Wu, B. Yu, and Y. Li. Design of retinal projection displays enabling vision correction. *Opt. Express*, 25(23):28223–28235, Nov 2017. doi: 10.1364/OE.25.028223

[4] J.-S. Chen and D. P. Chu. Improved layer-based method for rapid hologram generation and real-time interactive holographic display applications. *Optics Express*, 2015. doi: 10.1364/oe.23.018143

[5] D. Cheng, Y. Wang, H. Hua, and M. M. Talha. Design of an optical see-through head-mounted display with a low f-number and large field of view using a freeform prism. *Applied Optics*, 2009. doi: 10.1364/ao.48.002655

[6] D. Dunn, C. Tippets, K. Torell, P. Kellnhofer, K. Aksit, P. Didyk, K. Myszkowski, D. Luebke, and H. Fuchs. Wide Field of View Varifocal Near-Eye Display Using See-Through Deformable Membrane Mirrors. *IEEE Transactions on Visualization and Computer Graphics*, 23(4), 2017. doi: 10.1109/TVCG.2017.2657058

[7] Q. Gao, J. Liu, X. Duan, T. Zhao, X. Li, and P. Liu. Compact see-through 3D head-mounted display based on wavefront modulation with holographic grating filter. *Optics Express*, 2017. doi: 10.1364/OE.25.008412

[8] J. Geng. Three-dimensional display technologies. *Advances in Optics and Photonics*, 2013. doi: 10.1364/aop.5.000456

[9] Z. He, X. Sui, G. Jin, and L. Cao. Progress in virtual reality and augmented reality based on holographic display. *Applied Optics*, 2018. doi: 10.1364/ao.58.000a74

[10] D. M. Hoffman, A. R. Girshick, K. Akeley, and M. S. Banks. Vergence-accommodation conflicts hinder visual performance and cause visual fatigue. *Journal of Vision*, 2008. doi: 10.1167/8.3.33

[11] X. Hu and H. Hua. High-resolution optical see-through multi-focal-plane head-mounted display using freeform optics. *Optics Express*, 2014. doi: 10.1364/oe.22.013896

[12] H. Hua and B. Javidi. A 3D integral imaging optical see-through head-mounted display. *Optics Express*, 2014. doi: 10.1364/oe.22.013484

[13] F-C. Huang, K. Chen, and G. Wetzstein. The light field stereoscope. *ACM Transactions on Graphics*, 2015. doi: 10.1145/2766922

[14] C. Jang, K. Bang, S. Moon, J. Kim, S. Lee, and B. Lee. Retinal 3D: Augmented Reality Near-eye Display via Pupil-tracked Light Field Projection on Retina. *ACM Transactions on Graphics*, 2017. doi: 10.1145/3130800.3130889

[15] S.-B. Kim and J.-H. Park. Optical see-through Maxwellian near-to-eye display with an enlarged eyebox. *Optics Letters*, 2018. doi: 10.1364/ol.43.000767

[16] D. Lanman and D. Luebke. Near-eye light field displays. *ACM Transactions on Graphics*, 2013. doi: 10.1145/2508363.2508366

[17] C.-K. Lee, J.-Y. Hong, B. Lee, S. Lee, D. Yoo, and S. Moon. Compact three-dimensional head-mounted display system with Savart plate. *Optics Express*, 2016. doi: 10.1364/oe.24.019531

[18] J. S. Lee, Y. K. Kim, M. Y. Lee, and Y. H. Won. Enhanced see-through near-eye display using time-division multiplexing of a Maxwellian-view and holographic display. *Optics Express*, 2019. doi: 10.1364/oe.27.000689

[19] M. Liu, C. Lu, H. Li, and X. Liu. Near eye light field display based on human visual features. *Optics Express*, 2017. doi: 10.1364/oe.25.009886

[20] M. Liu, C. Lu, H. Li, and X. Liu. Bifocal computational near eye light field displays and Structure parameters determination scheme for bifocal computational display. *Optics Express*, 2018. doi: 10.1364/oe.26.004060

[21] S. Liu, D. Cheng, and H. Hua. An optical see-through head mounted display with addressable focal planes. In *Proceedings - 7th IEEE International Symposium on Mixed and Augmented Reality 2008, ISMAR 2008*, 2008. doi: 10.1109/ISMAR.2008.4637321

[22] G. D. Love, D. M. Hoffman, P. J. Hands, J. Gao, A. K. Kirby, and M. S. Banks. High-speed switchable lens enables the development of a volumetric stereoscopic display. *Optics express*, 2009. doi: 10.1364/OE.17.015716

[23] A. Maimone and H. Fuchs. Computational augmented reality eyeglasses. In *2013 IEEE International Symposium on Mixed and Augmented Reality, ISMAR 2013*, 2013. doi: 10.1109/ISMAR.2013.6671761

[24] A. Maimone, A. Georgiou, and J. S. Kollin. Holographic near-eye displays for virtual and augmented reality. *ACM Transactions on Graphics*, 2017. doi: 10.1145/3072959.3073624

[25] A. Maimone, D. Lanman, K. Rathinavel, K. Keller, D. Luebke, and H. Fuchs. Pinlight displays: wide field of view augmented reality eyeglasses using defocused point light sources. *international conference on computer graphics and interactive techniques*, 2014. doi: 10.1145/2601097.2601141

[26] H. Mukawa, K. Akutsu, I. Matsumura, S. Nakano, T. Yoshida, M. Kuwahara, and K. Aiki. A full-color eyewear display using planar waveguides with reflection volume holograms. *Journal of the Society for Information Display*, 2009. doi: 10.1889/JSID17.3.185

[27] K. Rathinavel, H. Wang, A. Blate, and H. Fuchs. An extended depth-at-field volumetric near-eye augmented reality display. *IEEE Transactions on Visualization and Computer Graphics*, 2018. doi: 10.1109/TVCG.2018.2868570

[28] J. P. Rolland, M. W. Krueger, and A. Goon. Multifocal planes head-mounted displays. *Applied Optics*, 39(19):3209, jul 2000. doi: 10.1364/AO.39.003209

[29] M. B. Spitzer, X. Miao, and B. Amirparviz. Method and apparatus for a near-to-eye display, feb 2013.

[30] P. Sun, S. Chang, S. Liu, X. Tao, C. Wang, and Z. Zheng. Holographic near-eye display system based on double-convergence light Gerchberg-Saxton algorithm. *Optics Express*, 2018.

[31] I. E. Sutherland. A head-mounted three dimensional display. In *Proceedings of the December 9-11, 1968, fall joint computer conference, part I*, pp. 757–764. ACM, 1968.

[32] H. Takahashi, Y. Ito, S. Nakata, and K. Yamada. Retinal projection type super multi-view head-mounted display. In *The Engineering Reality of*

Virtual Reality 2014, 2014. doi: 10.1117/12.2038330

[33] Y. Takaki and N. Fujimoto. Flexible retinal image formation by holographic Maxwellian-view display. *Optics Express*, 2018. doi: 10.1364/oe.26.022985

[34] G. Tan, T. Zhan, Y.-H. Lee, D. Zhao, S.-T. Wu, S. Liu, and J. Yang. Foveated imaging for near-eye displays. *Optics Express*, 2018. doi: 10.1364/oe.26.025076

[35] T. Ueno and Y. Takaki. Super multi-view near-eye display to solve vergenceaccommodation conflict. *Optics Express*, 2018. doi: 10.1364/oe.26.030703

[36] Y. Wang, J. Xie, Y. Chen, Z. Wu, Y. Liu, Y. Hu, H. Zhao, R. Shi, and J. Liu. Chromatic dispersion correction in planar waveguide using one-layer volume holograms based on three-step exposure. *Applied Optics*, 2012. doi: 10.1364/ao.51.004703

[37] Y. Wu, C. P. Chen, L. Mi, W. Zhang, J. Zhao, Y. Lu, W. Guo, B. Yu, Y. Li, and N. Maitlo. Design of retinal-projection-based near-eye display with contact lens. *Opt. Express*, 26(9):11553–11567, Apr 2018. doi: 10.1364/OE.26.011553

[38] A. Yuuki, K. Itoga, and T. Satake. A new Maxwellian view display for trouble-free accommodation. *Journal of the Society for Information Display*, 2012. doi: 10.1002/jsid.122

[39] J. Zhao, Q. Ma, J. Xia, J. Wu, B. Du, and H. Zhang. Hybrid computational near-eye light field display. *IEEE Photonics Journal*, 11(1):1–10, Feb 2019. doi: 10.1109/JPHOT.2019.2893934

[40] P. Zhou, Y. Li, S. Liu, and Y. Su. Compact design for optical-see-through holographic displays employing holographic optical elements. *Optics Express*, 2018. doi: 10.1364/oe.26.022866